Bioorganic & Medicinal Chemistry 18 (2010) 1273–1279

Contents lists available at ScienceDirect

Bioorganic & Medicinal Chemistry

journal homepage: www.elsevier.com/locate/bmc

A new series of flavones, thioflavones, and flavanones as selective monoamine oxidase-B inhibitors

Franco Chimenti [a], Rossella Fioravanti [a,*], Adriana Bolasco [a], Paola Chimenti [a], Daniela Secci [a], Francesca Rossi [a], Matilde Yáñez [b], Francisco Orallo [b], Francesco Ortuso [c], Stefano Alcaro [c], Roberto Cirilli [d], Rosella Ferretti [d], M. Luisa Sanna [d]

[a] Dipartimento di Chimica e Tecnologie del Farmaco, Università degli Studi di Roma "La Sapienza", P.le A. Moro 5, 00185 Roma, Italy
[b] Departamento de Farmacología and Instituto de Farmacia Industrial, Facultad de Farmacia, Universidad de Santiago de Compostela, Campus Universitario Sur, E-15782 Santiago de Compostela (La Coruña), Spain
[c] Dipartimento di Scienze Farmacobiologiche, Università di Catanzaro "Magna Graecia", "Complesso Ninì Barbieri", 88021 Roccelletta di Borgia (CZ), Italy
[d] Istituto Superiore di Sanità, Dipartimento del Farmaco, Viale Regina Elena 299, I-00161 Rome, Italy

ARTICLE INFO

Article history:
Received 2 November 2009
Revised 2 December 2009
Accepted 8 December 2009
Available online 4 January 2010

Keywords:
Flavones
MAO inhibitors
Molecular modeling
Enantiomeric separation

ABSTRACT

A new series of synthetic flavones, thioflavones, and flavanones has been synthesized and evaluated as potential inhibitors of monoamine oxidase isoforms (MAO-A and -B). The most active series is the flavanone one with higher selective inhibitory activity against MAO-B. Some of these flavanones (mainly the most effective) have been separated and tested as single enantiomers. In order to investigate the MAOs recognition of the most active and selective compounds, a molecular modeling study has been performed using available Protein Data Bank (PDB) structures as receptor models for docking experiments.

1. Introduction

Flavonoids are an extensive group of polyphenolic compounds present in plants, regularly consumed foods (e.g. vegetables and fruits), olive oil, and beverages like tea and wine.[1–3] They are usually subdivided, according to their chemical structure, into several subclasses including anthocyanidins, flavanones, flavones, flavonols, flavanonols (or dihydroflavonols), chalcones, isoflavones, and flavanols (flavan-3-ols) (also called catechins). Besides their physiological role in plants, these different flavonoids have been reported to possess a wide range of biological activities, including modulatory properties of several enzymes [e.g. activation of sirtuins,[4] inhibition of monoamine oxidase (MAO),[5] and a number of other biological activities such as anxiolytic,[6] anti-inflammatory,[3] antiviral,[7] antiprotozoal,[8] antioxidant,[3] cardiovascular,[3,9] and anti carcinogenic properties.[10–12]

Concerning the effects of flavonoids on the enzymatic activity of MAO (EC 1.4.3.4), several studies[5,13–15] have previously described the MAOIs (MAO Inhibitors) properties of jaceosidine, eupafolin, luteolin, quercetin, and apigenin (Chart 1).

Further in our recent paper[16] we have reported the activity of the flavone quercetin, which showed a selective MAO-A inhibitory activity in the nanomolar range (IC_{50} = 10 nM).

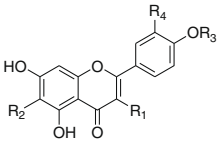

Luteolin = R_1= R_2= R_3= H, R_4= OH. (MAO-A IC_{50} 4.9 μM; MAO-B IC_{50} 59.7 μM)[5]
Quercetin = R_1=R_4= OH, R_2=R_3=H (MAO-A IC_{50} 2.8 μM; MAO-B IC_{50} 90.0 μM)[5]
Apigenin = R_1=R_2= R_3=R_4=H. (MAO-A IC_{50} 1.7 μM; MAO-B IC_{50} 12.8 μM)[5]
Jaceosidine = R_1=R_3=H, R_2=R_4=OCH_3. (MAO IC_{50} 19.0 μM)[14,15]
Eupafolin = R_1= OH, R_2= OCH_3, R_3= R_4= H. (MAO IC_{50} 25.0 μM)[14,15]

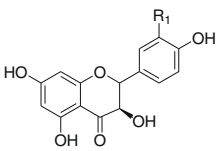

Taxifolin = R_1= OH (MAO IC_{50} 154.7 μM)[5]
Aromadendrin = R_1= H (MAO IC_{50} 153.1 μM)[5]

Chart 1. Natural flavonoids having inhibitory activity against MAO.

* Corresponding author. Tel.: +39 6 49693259; fax: +39 6 4462731.
E-mail address: rossella.fioravanti@uniroma1.it (R. Fioravanti).

0968-0896/$ - see front matter © 2009 Elsevier Ltd. All rights reserved.
doi:10.1016/j.bmc.2009.12.029

MAO is a flavoprotein located in the outer membrane of the mitochondria that contains a covalently bound flavin adenine dinucleotide (FAD) as a coenzyme and that has considerable physiological and pharmacological interest due to its central role in the metabolism of monoamine neurotransmitters. MAO exists in two isoforms, MAO-A and MAO-B, which share approximately 70% sequence identity on the amino acid levels and differ in their substrate specificity, susceptibility to specific inhibitors, and three-dimensional structure.[17,18] As indicated above, these MAO isoforms catalyze the biotransformation by oxidation of endogenous neurotransmitter monoamines and also the metabolization of various exogenous primary, secondary, and tertiary amines in the central nervous system as well as in peripheral tissues.[19] MAO-A preferentially deaminates 5-hydroxytryptamine (5-HT), norepinephrine, and epinephrine and is irreversibly inhibited by low concentrations of clorgyline whereas MAO-B preferentially deaminates dopamine, β-phenylethylamine, and benzylamine and is irreversibly inhibited by *R*-(−)-deprenyl.

It is well known that major depression is related to the deficit of monoamines (basically norepinephrine and 5-HT) at critical synapses in the central nervous system[20] whereas Parkinson's disease is mainly due to a deficit of dopamine.[21]

All these findings support the clinical importance of MAO inhibitors in the treatment of several neurological and psychiatric disorders. Thus, selective MAO-A inhibitors are used as anti-depressant and anti-anxiety drugs whereas selective MAO-B inhibitors can be mainly used to treat Parkinson's disease either alone or in combination with L-DOPA.[22,23]

Bearing in mind the above considerations, we consider that natural products as flavonoids (e.g. flavones and flavanones) are promising lead compounds for developing effective agents to combat neurological diseases. Therefore, as part of our continuous search for potential selective MAO inhibitors, we have synthesized flavones, thioflavones, and flavanones to investigate their inhibitory activity on human MAO isoforms (hMAO-A and -B). Due to the presence of a stereogenic carbon on the flavanone ring (flavanones exist as (*R*)- and (*S*)-enantiomers), we performed on the most active compounds the enantioseparation by chiral HPLC and tested the single enantiomers. Furthermore, the most promising compound binding mode to both hMAO-A and B catalytic clefts has been investigated by means of molecular modeling carried out using PDB crystallographic structures as receptor models for docking simulations.

2. Chemistry

The syntheses of the flavones and flavanones derivatives were carried out using chalcones as starting products[24,25]; (Scheme 1) whereas the thioflavones derivatives were prepared from the previously synthesized flavones. The synthesis of chalcone derivatives was performed according to procedures previously described.[26] Briefly, we used the aldolic condensation with $Ba(OH)_2{\cdot}8H_2O$ as base. In this process, 2′-hydroxyacetophenone reacted with an aldehyde. Chalcones **1a–p** and sodium acetate were heated in refluxing ethanol to obtain derivatives **2a–p**. To obtain derivatives 3a–**p** and **4a–p**, suitable chalcones **1a–p** were dissolved in DMSO (dimethyl sulfoxide) and iodine was added. After oxidative cyclization of chalcones, the derivatives **3a–p** were treated with Lawesson's reagent,[27] in refluxing benzene for 2 h to obtain **4a–p** derivatives.

3. Biochemistry

The potential effects of the test drugs on hMAO activity were investigated by measuring their effects on the production of hydrogen peroxide (H_2O_2) from *p*-tyramine (a common substrate for both hMAO-A and -B), using the Amplex Red MAO assay kit (Molecular Probes, Inc., Eugene, Oregon, USA) and microsomal MAO isoforms prepared from insect cells (BTI-TN-5B1-4) infected with recombinant baculovirus containing cDNA inserts for hMAO-A or -B (Sigma–Aldrich Química S.A., Alcobendas, Spain).

The production of H_2O_2 catalyzed by MAO isoforms, can be detected using 10-acetyl-3,7-dihydroxyphenoxazine (Amplex Red reagent), a non-fluorescent compound and highly sensitive probe that reacts with H_2O_2 in the presence of horseradish peroxidase to produce a fluorescent product, resorufin. In this study hMAO activity was evaluated using the above method following the general previously procedure described by.[28]

The test drugs (new compounds and reference inhibitors) themselves were unable to react directly with the Amplex Red reagent, which indicates that these drugs do not interfere with the measurements. On the other hand, in our experiments and under our experimental conditions, the control activity of hMAO-A and -B (using *p*-tyramine as a common substrate for both isoforms) was 165 ± 2 pmol of *p*-tyramine oxidized to *p*-hydroxyphenylacetaldehyde/min ($n = 20$).

Most tested flavonoids concentration-dependently and selectively inhibited the enzymatic control activity of MAO-B (see Tables 1–3).

4. Results and discussion

All synthesized compounds **2a–p**, **3a–p**, and **4a–p** were assayed for hMAO-A and -B inhibitory activity. By analyzing the data reported in Tables 1–3 it can be seen that the most active and hMAO-B selective compounds belong to flavanones **2a–p** derivatives and among them the best results (in the low micro molar range) were observed with compounds **2f**, **2g**, **2h**, **2j**, **2k**, and **2n**, substituted with the fluorine atom and the methyl or the methoxy group. It seems that the substitution pattern of these groups do not

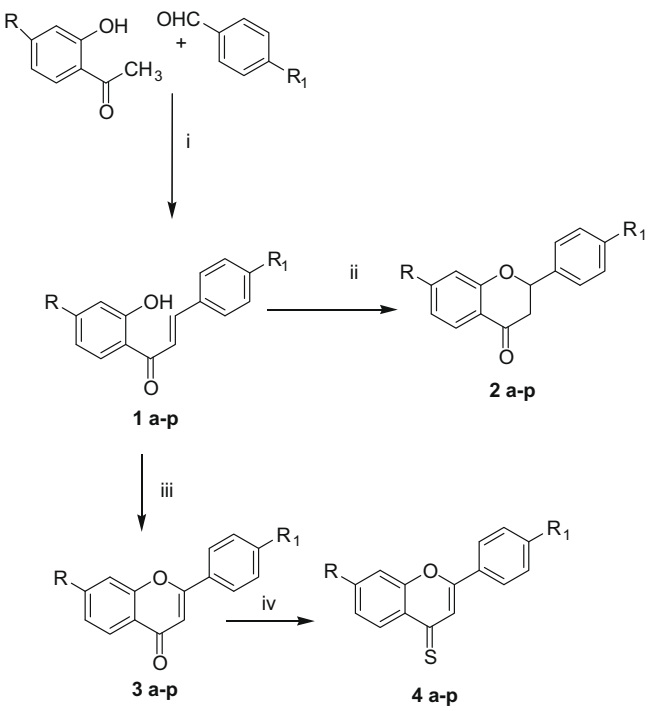

Scheme 1. Reagents and conditions: (i) $Ba(OH)_2{\cdot}8H_2O$, ethanol, 30 °C; (ii) CH_3COONa, ethanol, 24–48 h, reflux; (iii) I_2/DMSO, reflux; (iv) Lawesson's reagent, benzene, reflux, 2 h.

Table 1
Structures and inhibitory activity of derivatives **2a–p**

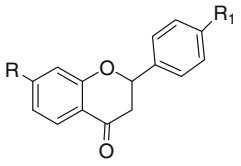

Compd	R	R_1	IC_{50} μM hMAO-A	IC_{50} μM hMAO-B	SI#
2a	H	H	**	2.87 ± 0.09	>35[b]
2b	H	F	**	4.41 ± 0.13	>23[b]
2c	H	CH_3	**	2.07 ± 0.11	>48b
2d	H	OCH_3	**	2.20 ± 0.10	>45[b]
2e	F	H	**	3.77 ± 0.16	>27[b]
2f	F	F	**	0.67 ± 0.04	>149[b]
2g	F	CH_3	**	0.16 ± 0.006	>625[b]
2h	F	OCH_3	**	0.17 ± 0.005	>588[b]
2i	CH_3	H	**	3.62± 0.10	>28[b]
2j	CH_3	F	**	0.13 ± 0007	>769[b]
2k	CH_3	CH_3	**	0.50 ± 0.02	>200[b]
2l	CH_3	OCH_3	**	3.35 ± 0.07	>30[b]
2m	OCH_3	H	**	1.47 ± 0.03	>68[b]
2n	OCH_3	F	**	0.17 ± 0.009	>588[b]
2o	OCH_3	CH_3	**	0.55 ± 0.02	>182[b]
2p	OCH_3	OCH_3	**	7.18 ± 0.06	>14[b]

Clorgyline (IC_{50} μM hMAO-A 0.004 ± 0.0003[a]; IC_{50} μM hMAO-B 61.35 ± 1.13; SI# 0.000065); *R*-(−)-deprenyl (IC_{50} μM hMAO-A 67.25 ± 1.02[a]; IC_{50} μM hMAO-B 0.019 ± 0.0009; SI# 3.539); Iproniazid (IC_{50} μM hMAO-A 6.56 ± 0.76; IC_{50} μM hMAO-B 7.54 ± 0.36; SI# 0.87); Moclobemide (IC_{50} μM hMAO-A 361.38 ± 19.37; IC_{50} μM hMAO-B *; SI# <0.36[c]); ≠SI: hMAO-B selectivity index = $IC_{50\ (hMAO\text{-}A)}/IC_{50\ (hMAO\text{-}B)}$. Each IC_{50} value is the mean ± S.E.M. from five experiments.
Level of statistical significance: [a]$P < 0.01$ versus the corresponding IC_{50} values obtained against hMAO-B, as determined by ANOVA/Dunnett's. [b]Values obtained under the assumption that the corresponding IC_{50} against hMAO-A is the highest concentration tested (100 μM). [c]Value obtained under the assumption that the corresponding IC_{50} against hMAO-B is the highest concentration tested (1 mM).
*Inactive at 1 mM (highest concentration tested).
** Inactive at 100 μM (highest concentration tested).

Table 2
Structures and inhibitory activity of derivatives **3a–p**

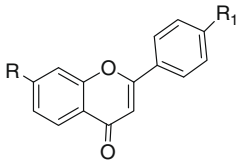

Compd	R	R_1	IC_{50} μM hMAO-A	IC_{50} μM hMAO-B	SI≠
3a	H	H	***	**	
3b	H	F	***	***	
3c	H	CH_3	**	2.38 ± 0.07	>42[b]
3d	H	OCH_3	***	27.87 ± 1.04	>3.6[b]
3e	F	H	***	12.94 ± 0.47	>7.7[b]
3f	F	F	**	***	
3g	F	CH_3	**	4.33 ± 0.39	>23[b]
3h	F	OCH_3	***	1.34 ± 0.02	>75[b]
3i	CH_3	H	**	**	
3j	CH_3	F	**	***	
3k	CH_3	CH_3	***	***	
3l	CH_3	OCH_3	***	***	
3m	OCH_3	H	**	***	
3n	OCH_3	F	**	5.14 ±0.18	>19[b]
3o	OCH_3	CH_3	**	11.34±0.26	>8.8[b]
3p	OCH_3	OCH_3	**	49.72±1.83	>2[b]

Clorgyline (IC_{50} μM hMAO-A 0.004 ± 0.0003a; IC_{50} μM hMAO-B 61.35 ± 1.13; SI# 0.000065); *R*-(−)-deprenyl (IC_{50} μM hMAO-A 67.25 ± 1.02[a]; IC_{50} μM hMAO-B 0.019 ± 0.0009; SI# 3.539); iproniazid (IC_{50} μM hMAO-A 6.56 ± 0.76; IC_{50} μM hMAO-B 7.54 ± 0.36; SI# 0.87); Moclobemide (IC_{50} μM hMAO-A 361.38 ± 19.37; IC_{50} μM hMAO-B*; SI# <0.36[c]); ≠SI: hMAO-B selectivity index = $IC_{50\ (hMAO\text{-}A)}/IC_{50\ (hMAO\text{-}B)}$. Each IC_{50} value is the mean ± S.E.M. from five experiments. Level of statistical significance: [a]$P < 0.01$ versus the corresponding IC_{50} values obtained against hMAO-B, as determined by ANOVA/Dunnett's. [b]Values obtained under the assumption that the corresponding IC_{50} against hMAO-A is the highest concentration tested (100 μM). [c]Value obtained under the assumption that the corresponding IC_{50} against hMAO-B is the highest concentration tested (1 mM).
*Inactive at 1 mM (highest concentration tested).
** Inactive at 100 μM (highest concentration tested).
*** 100 μM inhibits by approximately 40%.

affect the activity. The introduction of a double bond in the flavones **3a–p** and of the sulfur in the thioflavones **4a–p** leads to a relevant decrease of the inhibitory activity although remain a hMAO-B selectivity. The most active compounds **2f**, **2g**, **2h**, **2j**, **2k**, and **2n**, first assayed as racemates, were resolved by enantioselective HPLC and tested again as single enantiomers. The direct HPLC enantiomeric separation was accomplished on the immobilised polysaccharide-based Chiralpak IA chiral stationary phases (CSP) using pure methanol as a mobile phase. The absolute configuration of the enantiopure forms isolated at semipreparative scale was empirically assigned by comparing the circular dichroism (CD) spectra of the enantiomers of flavanone[29] with those of the structurally analogues **2f**, **2g**, **2h**, **2j**, **2k**, and **2n** (see Supplementary data).

In the reversibility and irreversibility tests, hMAO-B inhibition was irreversible in presence of the compounds selected for docking experiments [**2j**, (*R*)-**2j** and (*S*)-**2j**] (see below) as shown by the lack enzyme activity restoration after repeated washing. Similar results were obtained for *R*-(−)-deprenyl (Table 4). However, significant recovery of hMAO-A activity was observed after repeated washing of moclobemide, indicating that this drug is a reversible inhibitor of hMAO-A.

Compound **2j**, that evidenced the best inhibitory activity as racemate, was the best compound also in the two enantiomeric forms (Table 5). Because of this result we selected this compound for the subsequent molecular modeling investigation.

The recognition of both (*R*)-**2j** and (*S*)-**2j** enantiomers was evaluated by means of docking studies with respect to hMAO-A and -B receptor models. Two new, high resolution, PDB crystallographic structures, after a preliminary treatment, were adopted as targets (see Experimental section). The molecular modeling investigation, in qualitative agreement to the experimental data, reported the capability of both **2j** enantiomers to fit within hMAO-A and -B catalytic sites with some differences in terms of affinity. Actually both isomers recognized preferentially the hMAO-B binding cleft and, between them, the (*S*)-**2j** highlighted most favorable interactions.

In order to analyze the binding modes of **2j** enantiomers within the MAO isoforms, the most stable theoretical complexes were graphically inspected reporting similar interaction and binding modes.

Furthermore in Table 6 was reported the average *G* score values for the modeled compounds. As displayed in Figure 1 and according to interaction energy data, the (*R*)-**2j** showed a more productive recognition with respect to the (*S*)-**2j** into the hMAO-A. In the hMAO-A the (*R*)-**2j** was able to deeply penetrate into the active sites highlighting hydrophobic contacts to the FAD. Such an observation cannot be addressed to the (*S*)-**2j** located at a larger distance from the cofactor. Taking into account the orientation of both enantiomers into the hMAO-A binding cleft, (*S*)-**2j** appeared slightly translated toward the outer side. So, the most part of interacting residues was shared between the enantiomers but (*R*)-**2j** performed stronger interaction to Tyr407 and Tyr444 with respect to (*S*)-**2j** who, vice versa, was able to hydrophobically contact Ala111, Ile325, and Leu97.

A similar scenario was observed into the hMAO-B case but the binding mode differences were less remarkable (Fig. 2).

Although (*R*)-**2j** bound relatively deeper in the active site cavity, the (*S*)-enantiomer also was recognized by the FAD cofactor. The

Table 3
Structures and inhibitory activity of derivatives **4a–p**

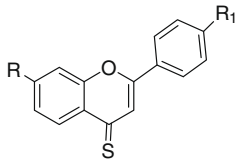

Compd	R	R_1	IC_{50}μM hMAO-A	IC_{50}μM hMAO-B	SI≠
4a	H	H	**	***	
4b	H	F	**	**	
4c	H	CH_3	**	6.69 ± 0.13	>15[b]
4d	H	OCH_3	***	0.48±0.024	>208[b]
4e	F	H	***	***	
4f	F	F	**	6.89 ± 0.19	>15[b]
4g	F	CH_3	***	1.61 ± 0.04	>62[b]
4h	F	OCH_3	**	***	
4i	CH_3	H	**	***	
4j	CH_3	F	**	***	
4k	CH_3	CH_3	**	6.72 ± 0.08	>15[b]
4l	CH_3	OCH_3	**	***	
4m	OCH_3	H	**	***	
4n	OCH_3	F	**	***	
4o	OCH_3	CH_3	***	7.61 ± 0.43	>13[b]
4p	OCH_3	OCH_3	**	3.34 ± 0.16	>30b

Clorgyline (IC_{50} μM hMAO-A 0.004 ± 0.0003a; IC_{50} μM hMAO-B 61.35 ± 1.13; SI# 0.000065); *R*-(−)-deprenyl (IC_{50} μM hMAO-A 67.25 ± 1.02[a]; IC_{50} μM hMAO-B 0.019 ± 0.0009; SI# 3.539); Iproniazid (IC_{50} μM hMAO-A 6.56 ± 0.76; IC_{50} μM hMAO-B 7.54 ± 0.36; SI# 0.87); Moclobemide (IC_{50} μM hMAO-A 361.38 ± 19.37; IC_{50} μM hMAO-B*; SI# <0.36[c]) SI: hMAO-B selectivity index = $IC_{50\ (hMAO-A)}/IC_{50\ (hMAO-B)}$. Each IC_{50} value is the means ± SEM from five experiments.
Level of statistical significance: [a]$P < 0.01$ versus the corresponding IC_{50} values obtained against hMAO-B, as determined by ANOVA/Dunnetťs. [b]Values obtained under the assumption that the corresponding IC_{50} against hMAO-A is the highest concentration tested (100 μM). [c]Value obtained under the assumption that the corresponding IC_{50} against hMAO-B is the highest concentration tested (1 mM).
*Inactive at 1 mM (highest concentration tested).
** Inactive at 100 μM (highest concentration tested).
*** 100 μM inhibits by approximately 40%.

number of interacting residues was equivalent and a large part of them was shared. So the slightly advantage of (*S*)-**2j** interaction energy with respect to (*R*)-**2j** could be addressed to the better accommodation of its fluorophenyl moiety into the lipophilic cage delimited by Trp119, Phe168, Leu171, Ile199, and Tyr326. The analysis of the residues involved in the recognition of **2j** enantiomers in both MAO isoforms revealed that the selectivity was not addressed to canonical differences between the catalytic gorges such as Ile199 and Tyr326 (hMAO-B), respectively, versus Phe208 and Ile335 (hMAO-A).

Actually all these crucial amino acids interacted with both **2j** enantiomers as shown in Figures 1 and 2. Since the average *G* score values (see Table 6) take into account other effects (solvation, penalty clashes, loss of ligand internal degrees of freedom, etc) the hMAO-B selectivity can be addressed to those terms. Finally in order to clarify the role of R_1 we have compared the hMAO-B

Table 5
Inhibitory activity of single enantiomer of the most active flavanones **2**

Comp.	IC_{50} μM hMAO-A	IC_{50} μM hMAO-B	SI[a]
(*R*)(+)**2f**	**	0.65 ± 0.03	>154[b]
(*S*)(-)**2f**	**	0.62 ± 0.02	>161[b]
(*R*)(+)**2g**	**	0.15 ± 0.01	>667[b]
(*S*)(−)**2g**	**	0.17 ± 0.01	>588[b]
(*R*)(+)**2h**	**	0.15 ± 0.01	>667[b]
(*S*)(−)**2h**	**	0.15 ± 0.01	>667[b]
(*R*)(+)**2j**	**	0.14 ± 0.01	>714[b]
(*S*)(−)**2j**	**	0.11 ± 0.01	>909[b]
(*R*)(+)**2k**	**	0.53 ± 0.03	>189[b]
(*S*)(−)**2k**	**	0.59 ± 0.03	>169[b]
(*R*)(+)**2n**	**	0.20 ± 0.01	>500[b]
(*S*)(−)**2n**	**	0.16 ± 0.01	>625[b]

Each IC_{50} value is the means ± SEM from five experiments.
[a] SI: hMAO-B selectivity index = $IC_{50\ (hMAO-A)}/IC_{50\ (hMAO-B)}$.
[b] Values obtained under the assumption that the corresponding IC_{50} against MAO-A is the highest concentration tested (100 μM).

Table 6
Theoretical affinity of **2j**, (*R*)-**2j**, and (*S*)-**2j** with respect to MAO isoforms

Comp	hMAO-A*	hMAO-B*
(±)-**2j**	−6.75	−7.45
(*R*)-**2j**	−6.93	−7.44
(*S*)-**2j**	−6.58	−7.47

* Average *G* score values.

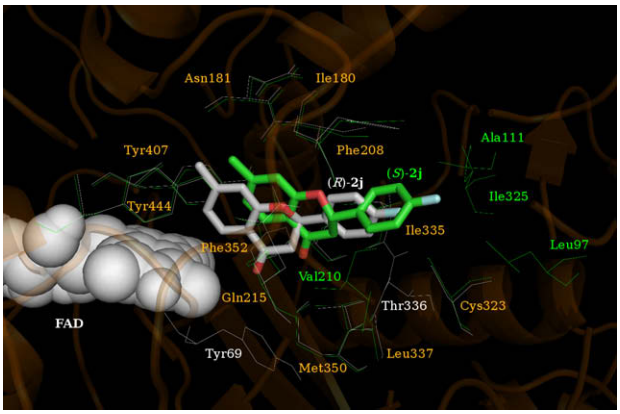

Figure 1. Superimposition of best fully energy minimized hMAO-A poses of (*R*)-**2j** and (*S*)-**2j**. The ligand is reported as white and green carbon polytube, respectively. The interacting residues with (*R*)-**2j** and (*S*)-**2j** are colored in white and green, respectively. The FAD cofactor is displayed as a spacefill structure. Non-polar hydrogen atoms are omitted for clarity.

Table 4
Reversibility and irreversibility of hMAO inhibition of compound **2j** and of its separated enantiomers

Compd	% hMAO-A inhibition		% hMAO-B inhibition	
	Before washing	After repeated washing	Before washing	After repeated washing
(*R*)(−)**D**[a] (20 nM)			51.45 ± 2.69	52.05 ± 2.88
M[a] (500 μM)	84.75 ± 4.34	10.26 ± 0.65[b]		
2j (100 nM)			38.36 ± 3.15	36.51 ± 2.56
(*R*)(+)**2j** (100 nM)			35.61 ± 2.90	37.23 ± 3.14
(*S*)(−)**2j** (100 nM)			45.29 ± 3.92	42.58 ± 3.37

[a] **D**, (*R*)(−)deprenyl; **M**, moclobemide. Each value is the means ± SEM from five experiments ($n = 5$).
[b] Level of statistical significance: $P < 0.01$ versus the corresponding % hMAO-A inhibition before washing, as determined by ANOVA/Dunnetťs.

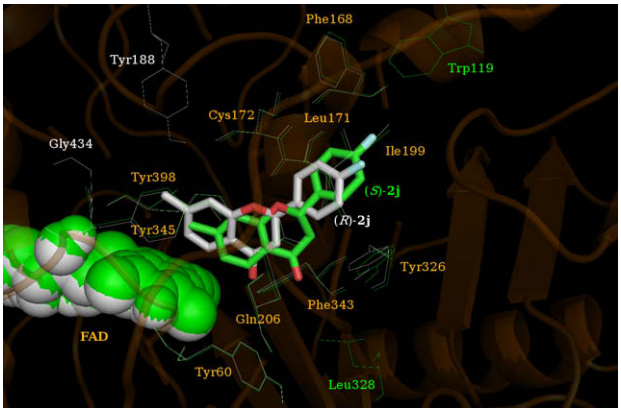

Figure 2. Superimposition of best fully energy minimized hMAO-B poses of (*R*)-**2j** and (*S*)-**2j**. The ligand is reported as white and green carbon polytube, respectively. The interacting residues with (*R*)-**2j** and (*S*)-**2j** are colored in white and green, respectively. The FAD cofactor is displayed as a spacefill structure. Non-polar hydrogen atoms are omitted for clarity.

interaction energies of **2j**, **2i**, **2k**, and **2l** averaging the values of both enantiomers. The results (not shown) indicated the fluorophenyl as the best moiety with the optimal compromise of lipophilicity and steric hindrance. In principle, our results of irreversibility obtained with the compounds **2j**, (*R*)-**2j**, and (*S*)-**2j**, do not seem to correlate well with the conformational analysis made in the docking studies but a number of arguments may explain, at least in part, this discrepancy. In most cases, the irreversible inhibitors establish a covalent interaction with the active center of the enzyme.[30]

However, not all irreversible inhibitors form covalent adducts with their enzyme targets but they may also act by other mechanisms. In fact, some reversible inhibitors bind so tightly to their target enzyme that they are essentially irreversible. These tight-binding inhibitors may show kinetics similar to covalent irreversible inhibitors. In these cases, some of these inhibitors rapidly bind to the enzyme in a low-affinity enzyme-inhibitor (EI) complex and this then undergoes a slower rearrangement to a very tightly bound EI* complex. This kinetic behavior is called slow-binding. This slow rearrangement after binding often involves a conformational change as the enzyme "clamps down" around the inhibitor molecule.[31] In contrast, some irreversible MAO inhibitors (the so-called suicide inhibitors) act as a substrate for the target enzyme, which finally generates a new compound that irreversibly inhibits MAO activity. Therefore, the initial interaction of these inhibitors with MAO may be different to the interaction obtained after several minutes of the enzyme–inhibitor complex formation (see above). *R*-(−)-deprenyl, for example, first of all form a non-covalent complex with MAO as an initial, reversible step. The subsequent interaction of *R*-(−)-deprenyl with MAO leads to a reduction of the enzyme-bound FAD, and concomitant oxidation of the inhibitor. This oxidized inhibitor then reacts with FAD at the N-5-position in a covalent manner.[32] The initial non-covalent binding to MAO has been also described for other MAO inhibitors (e.g. clorgyline derivatives).[33] Finally, it is possible that, in some cases of irreversible inhibition, a steric hindrance may prevent the release of the inhibitor from the enzymatic active center (although its interaction with this binding site is either very weak or reversible).

Bearing in mind all the above considerations and taking into account that the docking studies make only a theoretical prediction of the initial possible interaction inhibitor–enzyme, the results obtained in these docking studies and in the reversibility experiments may be different.

5. Experimental

5.1. General procedure for the synthesis of 2′-hydroxy chalcones 1a–p

A solution of suitable 2-hydroxy acetophenone (0.01 mol) and the suitable benzaldehyde (0.01 mol) dissolved in ethanol was treated with barium hydroxide (0.01 mol). The solution was stirred for 24 h at 30 °C. After the pH of the reaction mixture was brought back to 7.0 by the careful addition of HCl 1 N solution. The aqueous layer was extracted with ethyl acetate, washed with brine, dried (Na_2SO_4), and then concentrated in vacuo. The residue was purified by crystallization from ethanol, to afford chalcones **1a–p**.

5.2. General procedure for the synthesis of flavanones 2a–p

Chalcones **1a–p** (0.2 mmol) and sodium acetate (2.0 mmol) were heated in refluxing ethanol (2 mL) for 24–48 h. The mixture was then allowed to cool to r.t. and poured into ice water (10 mL) and extracted with CH_2Cl_2 (3 × 10 mL). The combined organic phase was washed with brine, dried over Na_2SO_4, and then concentrated in vacuo. The residue was column chromatographed on silica gel, eluting with mixture of ethyl acetate/hexane 1:4, to afford flavanones **2a–p** which were crystallized from suitable solvent (see Supplementary data).

5.3. General procedure for the synthesis of flavones 3a–p

To a solution of chalcones **1a–p** (0.015 moL) in 50 ml of DMSO (dimethyl sulfoxide) were added iodine (0.015 mol). The reaction mixture was stirred for 30 min at 130 °C. Then the mixture was treated with sodium thiosulfate (solution 20%) and extracted with $CHCl_3$ (3 × 10 mL). The combined organic phase were washed with brine, dried over Na_2SO_4, and then concentrated in vacuo. The residue was purified by crystallization from suitable solvent (see Supplementary data).

5.4. General procedure for the synthesis of thioflavones 4a–p

A 100 mL flask was charged with flavones **3a–p** (0.05 mol) and Lawesson's reagent (0.025 mol), whereupon the temperature of the reaction mixture increases to 78–80 °C. After 5 min, 35 mL of benzene was added, the mixture was heated at refluxing for 2 h, then was cooled to r.t., and the solvent removed under vacuum. The crude solid was purified by suitable method (see Supplementary data).

5.5. Determination of hMAO isoform activity

The effects of the test compounds on hMAO isoform enzymatic activity were evaluated by a fluorimetric method following the experimental protocol previously described.[28]

Briefly, 0.1 mL of sodium phosphate buffer (0.05 M, pH 7.4) containing various concentrations of the test drugs (new compounds or reference inhibitors) and adequate amounts of recombinant hMAO-A or -B required and adjusted to obtain in our experimental conditions the same reaction velocity, i.e., to oxidize (in the control group) 165 pmol of *p*-tyramine/min (hMAO-A: 1.1 μg protein; specific activity: 150 nmol of *p*-tyramine oxidized to *p*-hydroxyphenylacetaldehyde/min/mg protein; hMAO-B: 7.5 μg protein; specific activity: 22 nmol of *p*-tyramine transformed/min/mg protein) were incubated for 15 min at 37 °C in a flat-black-bottom 96-well microtest plate (BD Biosciences, Franklin Lakes, NJ, USA) placed in the dark multimode microplate reader chamber. After this incubation period, the reaction was started by adding (final

concentrations) 200 μM Amplex Red reagent, 1 U/ml horseradish peroxidase and 1 mM *p*-tyramine. The production of H_2O_2 and, consequently, of resorufin was quantified at 37 °C in a multimode microplate reader (Fluostar Optima, BMG Labtech GmbH, Offenburg, Germany), based on the fluorescence generated (excitation, 545 nm, emission, 590 nm) over a 15 min period, in which the fluorescence increased linearly.

Control experiments were carried out simultaneously by replacing the test drugs (new compounds and reference inhibitors) with appropriate dilutions of the vehicles. In addition, the possible capacity of the above test drugs to modify the fluorescence generated in the reaction mixture due to non-enzymatic inhibition (e.g. for directly reacting with Amplex Red reagent) was determined by adding these drugs to solutions containing only the Amplex Red reagent in a sodium phosphate buffer.

The specific fluorescence emission (used to obtain the final results) was calculated after subtraction of the background activity, which was determined from vials containing all components except the MAO isoforms, which were replaced by a sodium phosphate buffer solution.

5.6. Reversibility and irreversibility experiments

To evaluate whether some of the tested compounds, **2j**, (*R*)-**2j**, and (*S*)-**2j**, are reversible or irreversible hMAO-B inhibitors, an effective centrifugation–ultrafiltration method (so-called repeated washing) previously described was used.[26]

Briefly, adequate amounts of the recombinant hMAO-B were incubated together with a single concentration (see Table 4) of the test drugs or the reference inhibitor *R*-(−)-deprenyl in a sodium phosphate buffer (0.05 M, pH 7.4) for 15 min at 37 °C.

Then, an aliquot of this incubated was stored at 4 °C and used for subsequent measurement of hMAO-B activity under the experimental conditions indicated above (see the subsection determination of MAO activity). The remaining incubated sample (300 μL) was placed in a Ultrafree-0.5 centrifugal tube (Millipore, Billerica, USA) with a 30 kDa Biomax membrane in the middle of the tube and centrifuged (9000*g*, 20 min, 4 °C) in a centrifuge (J2-MI, Beckman Instruments, Inc., Palo Alto, California, USA). The enzyme retained in the 30 kDa membrane was resuspended in sodium phosphate buffer at 4 °C and centrifuged again (under the same experimental conditions described above) two successive times. After the third centrifugation, the enzyme retained in the membrane was resuspended in sodium phosphate buffer (300 μL) and an aliquot of this suspension was used for subsequent hMAO-B activity determination.

Similar studies were carried out on hMAO-A activity in presence of the reference inhibitor moclobemide under the experimental conditions described above.

Control experiments were performed simultaneously (to define 100% hMAO activity) by replacing the test drugs with appropriate dilutions of the vehicles. The corresponding values of percent (%) hMAO inhibition were separately calculated for samples with and without repeated washing.

6. Enantioseparation studies

HPLC enantioseparations were performed by using stainless-steel Chiralpak IA (250 × 4.6 mm I.D. and 250 × 10 mm I.D.) (Daicel, Chemical Industries, Tokyo, Japan) columns. HPLC-grade solvents were supplied by Carlo Erba (Milan, Italy). HPLC apparatus consisted in a Perkin–Elmer (Norwalk, CT, USA) 200 lc pump equipped with a Rheodyne (Cotati, CA, USA) injector, a HPLC Dionex (CA, USA) Model TCC-100 oven and a Jasco (Jasco, Ishikawacho, Hachioji City, Tokyo, Japan) Model 2095 Plus UV/CD detector. The mobile phases were filtered and degassed by sonication immediately before using. In analytical enantioseparations, standard solutions were prepared by dissolving about 1 mg of racemic sample, into 10 ml of methanol. The injection volume was 10–20 μl. In a semipreparative enantioseparation 1 mL sample loop was used. After semipreparative separation, the collected fractions were analyzed by chiral analytical columns to determine their enantiomeric excess (ee).

The column hold-up time (t_0 = 3.0 min for the 250 × 4.6 mm i.d. column) was determined from the elution of an unretained marker (toluene), using methanol as eluent, delivered at a flow-rate of 1.0 mL/min.

The chromatographic and polarimetric data of the enantiomers separated at semipreparative scale are summarized in Supplementary data, Table 4. Specific rotations were measured at 589 nm by a Perkin-Elmer polarimeter model 241 equipped with a Na lamp. The volume of the cell was 1 mL and the optical path was 10 cm. The system was at a temperature of 20 °C by a Neslab RTE 740 cryostat. The circular dichroism (CD) spectra of the enantiomers of **2f**, **2g**, **2h**, **2j**, **2k**, and **2n**, dissolved in ethanol (concentration about 0.2 mg/mL), in a quartz cell (0.1 cm-path length) at 25 °C, were measured by using a Jasco Model J-700 spectropolarimeter (see Supplementary data, Fig. 1). The spectra are average computed over three instrumental scans and the intensities are presented in terms of ellipticity values (mdeg).

7. Molecular modeling

The Protein Data Bank[34] (PDB) crystallographic structures 2Z5X[35] and 2BK3[36] were considered as receptor model of hMAO-A and -B, respectively.

Both (*R*) and (*S*) enantiomers of **2j** were built by means of the Maestro GUI[37] and energy minimized using the OPLS-AA[38] force field as implemented in Macromodel ver. 7.2.[39] Water solvent effects were taken into account using the implicit solvation model GB/SA.[40] The optimized structures were submitted to docking simulations with respect to hMAO-A and -B PDB crystallographic structures. Both receptor models required graphical manipulation: the co-crystallized ligands, harmine and farnesol, respectively, for 2Z5X and 2BK3, were removed, FAD double bonds were corrected, and hydrogen atoms were added onto both proteins and cofactors.

According to the Glide[41] methodology, a regular box, of about 110,000 $Å^3$, centered onto the cofactor N5 atom, was considered as the enzyme active site for both hMAO-A and -B models. In order to take into account the induced fit phenomena, **2j** enantiomers were docked using the Glide "flexible" algorithm. The binding affinity has been evaluated using the *G* Score average value computed from the ten best generated poses for each enantiomer into the hMAO-A and –B, respectively (see Supplementary data). The most stable complexes were submitted to energy minimization using the same force field and aqueous environment previously reported. The resulting optimized structures were considered for the binding modes graphical analysis. PyMol ver. 0.98[42] was used to create Figs. 1 and 2.

The results obtained in this study indicate that flavonoids may have interesting therapeutic potential as original chemical models (templates) for the design and subsequent development of new drugs (selective and efficient MAO-B inhibitors) useful for improving the pharmacological treatment of neurodegenerative diseases (e.g. Parkinson's disease).

Acknowledgments

This work was supported by Grants from MURST (Italy). Ministerio de Sanidad y Consumo (Spain; FISS PI061537) and Consellería

de Innovación e Industria de la Xunta de Galicia (Spain; INCITE07PXI203039ES, INCITE08E1R203054ES and 08CSA019203PR).

Supplementary data

Supplementary data associated with this article can be found, in the online version, at doi:10.1016/j.bmc.2009.12.029.

References and notes

1. Harborne, J. B.; Baxter, H. Ed.; The Handbook of Natural Flavonoids; 1999; Vol. 2, pp 879–889.
2. Aherne, S. A.; O'Brien, N. M. *Nutrition* **2002**, *18*, 75.
3. Middleton, E., Jr.; Kandaswami, C.; Theoharides, T. C. *Pharmacol. Rev.* **2000**, *52*, 673.
4. Orallo, F. *Curr. Med. Chem.* **2008**, *15*(19), 1887.
5. Hua Han, X.; Su Hong, S.; Hwang, J. S.; Koo Lee, M.; Hwang, B. Y.; Seup Ro, J. *Arch. Pharm. Res.* **2007**, *30*, 13.
6. Marder, M.; Paladini, A. C. *Curr. Top. Med. Chem.* **2002**, *2*, 853.
7. Manthey, J. A.; Grohmann, K.; Guthrie, N. *Curr. Med. Chem.* **2001**, *8*, 135.
8. Fournet, A.; Munoz, V. *Curr. Top. Med. Chem.* **2002**, *2*, 1215.
9. Manach, C.; Mazur, A.; Scalbert, A. *Curr. Opin. Lipidol.* **2005**, *16*, 77.
10. (a) Cardenas, M.; Marder, M.; Blank, V. C.; Roguin, L. P. *Bioorg. Med. Chem.* **2006**, *14*, 2966. and references therein; (b) Akama, T.; Shida, Y.; Sugaya, T.; Ishida, H.; Gomi, K.; Kasai, M. J. *J. Med. Chem.* **1996**, *39*, 3461; (c) Cushman, M.; Nagarathnam, D. J. *Nat. Prod.* **1991**, *54*, 1656; (d) Hayashi, T.; Uchida, K.; Hayashi, K.; Niwayama, S.; Morita, N. *Chem. Pharm. Bull.* **1988**, *36*, 4849; (e) Beutler, J. A.; Cardellina, J. H., II; Lin, C. M.; Hamel, E.; Cragg, G. M.; Boyd, M. R. *Bioorg. Med. Chem. Lett.* **1993**, *3*, 581.
11. Li, Y.; Fang, H.; Xu, W. *Mini Rev. Med. Chem.* **2007**, *7*(7), 663.
12. Shankar, S.; Ganapathy, S.; Srivastava, R. K. *Front Biosci.* **2007**, *12*, 4881.
13. Singh, A.; Naidu, P. S.; Kulkarni, S. K. *Pharmacology* **2003**, *68*, 81.
14. Lee, S. J.; Chung, H. Y.; Lee, I. K.; Oh, S. U.; Yoo, I. D. *Food Sci. Biotechnol.* **2000**, *9*, 179.
15. Brahmachari, G.; Gorai, D. *Curr. Org. Chem.* **2006**, *10*, 873.
16. Chimenti, F.; Cottiglia, F.; Bonsignore, L.; Casu, L.; Casu, M.; Floris, C.; Secci, D.; Bolasco, A.; Chimenti, P.; Granese, A.; Befani, O.; Turini, P.; Alcaro, S.; Ortuso, F.; Trombetta, G.; Loizzo, A.; Guarino, I. J. *Nat. Prod.* **2006**, *69*, 945.
17. Binda, C.; Hubálek, F.; Li, M.; Edmondson, D. E.; Mattevi, A. *FEBS Lett.* **2004**, *564*(3), 225.
18. Edmondson, D. E.; Mattevi, A.; Binda, C.; Li, M.; Hubalek, F. *Curr. Med. Chem.* **2004**, *11*, 1983.
19. Kopin, I. J. *Pharmacol. Rev.* **1985**, *37*, 338.
20. Schildkraut, J. J. *Am. J. Psychiatry* **1965**, *122*, 509.
21. Grimbergen, Y. A.; Langston, J. W.; Roos, R. A.; Bloem, B. R. *Expert Rev. Neurother.* **2009**, *9*(2), 279.
22. Henchcliffe, C.; Schumacher, H. C.; Burgut, F. T. *Expert. Rev. Neurother.* **2005**, *5*, 811.
23. Youdim, M. B.; Edmondson, D.; Tipton, K. F. *Nat. Rev. Neurosci.* **2006**, *7*, 295.
24. Lim, S. S.; Jung, S. H.; Ji, J.; Shin, K. H.; Keum, S. R. J. *J. Pharm. Pharmacol.* **2001**, *53*, 653.
25. Fukai, T.; Nomura, T. *Heterocycles* **1991**, *32*(3), 499.
26. Chimenti, F.; Fioravanti, R.; Bolasco, A.; Chimenti, P.; Secci, D.; Rossi, F.; Yanez, M.; Orallo, F.; Ortuso, F.; Alcaro, S. J. *Med. Chem.* **2009**, *52*(9), 2818.
27. Levai, A. *Heterocyclic Commun.* **1999**, *5*, 419.
28. Chimenti, F.; Secci, D.; Bolasco, A.; Chimenti, P.; Bizzarri, B.; Granese, A.; Carradori, S.; Yanez, M.; Orallo, F.; Ortuso, F.; Alcaro, S. J. *Med. Chem.* **2009**, *52*(9), 1935.
29. Cirilli, R.; Ferretti, R.; De Santis, E.; Gallinella, B.; Zanitti, L.; La Torre, F. J. *Chromat A* **2008**, *1190*(1–2), 95.
30. Tipton, K. F.; Boyce, S.; O'Sullivan, J.; Davey, G. P.; Healy, J. *Curr. Med. Chem.* **2004**, *11*, 1965.
31. Szedlacsek, S. E.; Duggleby, R. G. *Meth. Enzymol.* **1995**, *249*, 144.
32. Gerlach, M.; Riederer, P.; Youdim, M. B. *Eur. J. Pharmacol.* **1992**, *226*, 97.
33. O'Brien, E. M.; Tipton, K. F.; Meroni, M.; Dostert, P. J. *Neural. Transm. Suppl.* **1994**, *41*, 295.
34. Berman, H. M.; Westbrook, J.; Feng, Z.; Gilliland, G.; Bhat, T. N.; Weissig, H.; Shindyalov, I. N.; Bourne, P. E. *Nucleic Acids Res.* **2000**, *28*, 235.
35. Son, S. Y.; Ma, J.; Kondou, Y.; Yoshimura, M.; Yamashita, E.; Tsukihara, T. *Proc. Natl. Acad. Sci. USA* **2008**, *105*, 5739. Data deposition: www.pdb.org (PDB ID code2Z5X).
36. Hubalek, F.; Binda, C.; Khalil, A.; Li, M.; Mattevi, A.; Castagnoli, N.; Edmondson, D. E. *J. Biol. Chem.* **2005**, *280*, 15761. Data deposition: www.pdb.org (PDB ID code 2BK3).
37. Maestro ver. 4.1 Schroedinger Inc.: Portland, OR, 1998–2001.
38. Kaminski, G.; Friesner, R. A.; Tirado-Rives, J.; Jorgensen, W. L. J. *Phys. Chem. B* **2001**, *105*, 6474.
39. Mohamadi, F.; Richards, N. G. J.; Guida, W. C.; Liskamp, R.; Lipton, M.; Caufield, C.; Chang, G.; Hendrickson, T.; Still, W. C. J. *Comput. Chem.* **1990**, *11*, 440.
40. Hasel, W.; Hendrickson, T. F.; Still, W. C. *Tetrahedron Comput. Methodol.* **1988**, *1*, 103.
41. [a] Glide ver. 4.1, Schroedinger Inc.: Portland, OR, 1998–2001.; (b) Eldridge, M. D.; Murray, C. W.; Auton, T. R.; Paolini, G. V.; Mee, R. P. *J. Comput. Aided Mol. Des.* **1997**, *11*, 425.
42. DeLano, W. L. The PyMOL Molecular Graphics System; DeLano Scientific: San Carlos, CA, 2002. http://www.pymol.org.